

Continuous Low Temperature Synthesis of MAPbX₃ Perovskite Nanocrystals in a Flow Reactor

Xinxing Liang,^a Kejun Wu,^b Wentao Deng,^a Robert Baker,^a Dominic Ferdani,^a Peter. S. Kubiak^a Frank Marken,^a Laura Torrente-Murciano^b and Petra J Cameron^{*a}

Experimental

Materials. Lead (II) iodide (PbI₂, 99%, Aldrich), lead (II) bromide (PbBr₂, 99.999%, Aldrich), octadecene (ODE, 90%, Acros Organics), methylammonium iodide (MAI, Dyesol), methylammonium bromide (MABr, Dyesol), 1-butanol (BuOH, 99%, Acros Organics), oleylamine (OLA, 80%-90%, Acros Organics), oleic acid (OA, 90%, Alfa Aesar), toluene (ACS reagent, VWR International), N,N-dimethylformamide (DMF, anhydrous, 99.8%, Sigma-Aldrich). All reagents and solvents were used as received without further purification.

Synthesis of MAPbX₃ NCs. 0.8 mmol PbI₂ or PbBr₂ was added in 8 mL ODE with 1.2 mL OLA and 1.2 mL OA, and heated to 100 °C to dissolve. 0.8 mmol MAI or MABr was dissolved in the mixture of 8 mL 1-BuOH and 4 mL ODE with 1 mL OA. For MAPbI₃ synthesis, the PbI₂ solution and MAI solution were pumped using syringe pumps and mixed in a T-junction with a molar ratio of 1:1 before being flown through a 3 meter PTFE tubing (1.5 mm ID) reactor in a water bath of 30 °C, as shown in **Figure 1**. The flow rates of the two solutions were set to be 236 uL/min and 294 uL/min respectively, resulting in a residence time of 10 min. The mixture was collected in a container sitting inside an ice bath to help quench the reaction. The final product was centrifuged and the supernatant containing any unreacted precursors was discarded. The solid was re-dispersed in toluene. In some cases a second centrifugation step was used to remove any larger aggregates. For MAPbI_xBr_{3-x} NCs, the PbI₂ solution was replaced by the mixture of PbI₂ solution and PbBr₂ solution, and/or MAI solution was replaced by the mixture of MAI solution and MABr solution, according to the ratio of I:Br=x:(3-x).

Synthesis of bulk MAPbI₃ powder and film. PbI₂ and CH₃NH₃I were dissolved in DMF and stirred at 60 °C for an hour. To make the MAPbI₃ powder, the solution was cast onto a clean glass petri dish at 100 °C and left for an hour. To prepare the MAPbI₃ films, the solution was spin-coated onto clean 2.5 cm × 2.5 cm FTO substrates at 3000 rpm for 30 s followed by annealing at 100 °C for 30 min.

Photoluminescence. Photoluminescence spectra were obtained on a Gilden photonics fluoroSENS fluorimeter. The dispersions of MAPbX₃ NCs and bulk MAPbI₃ powder in toluene were put in a 1-cm quartz cuvette and excited at 365 nm. The integrating time was 100 ms. All the data were obtained at room temperature and under air atmosphere.

UV-visible measurement. UV-vis spectra of the MAPbX₃ NCs dispersed in toluene were measured using a quartz cuvette on a Varian Cary 50 UV-Visible spectrophotometer. Scans were carried out at a rate of 300 nm/min at room temperature.

X-ray diffraction (XRD). Clean silicon wafers were immersed in the dispersion of MAPbX₃ NCs in toluene. After 48h, the wafers were taken out and blow-dried with nitrogen flow. XRD spectra of the NC films and the MAPbI₃ bulk film were measured using a BRUKER D8-Advance Powder X-Ray

Diffraction pattern was scanned over the angular range of 5-40 degree (2θ) with a step size of 0.023 and a rotation speed of 15 rpm, at room temperature.

Transmission electron microscopy (TEM). TEM measurements were carried out to investigate the micromorphology of the MAPbX_3 NCs. The samples were prepared by dropping the toluene dispersions of the NCs onto carbon supported copper grids followed by drying overnight under vacuum. The TEM measurements were performed on a JEOL JEM-2100Plus transmission electron microscope with an acceleration voltage of 200 kV.

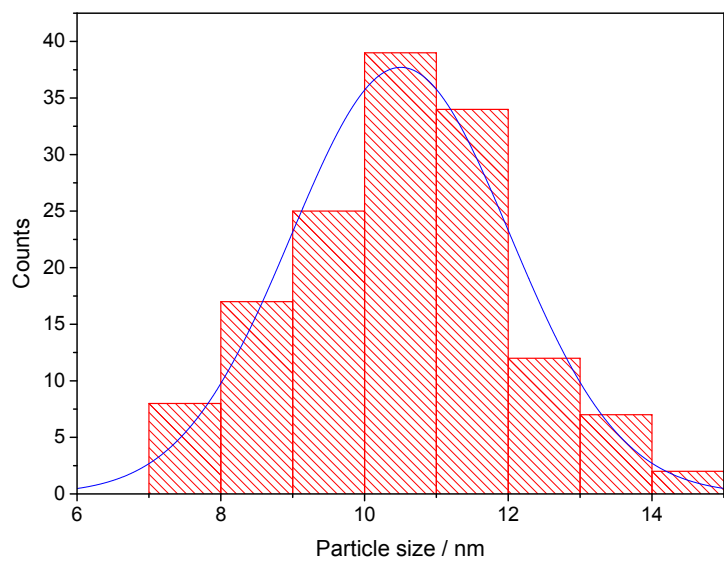


Figure S1. Size distribution of MAPbI₃ NCs.

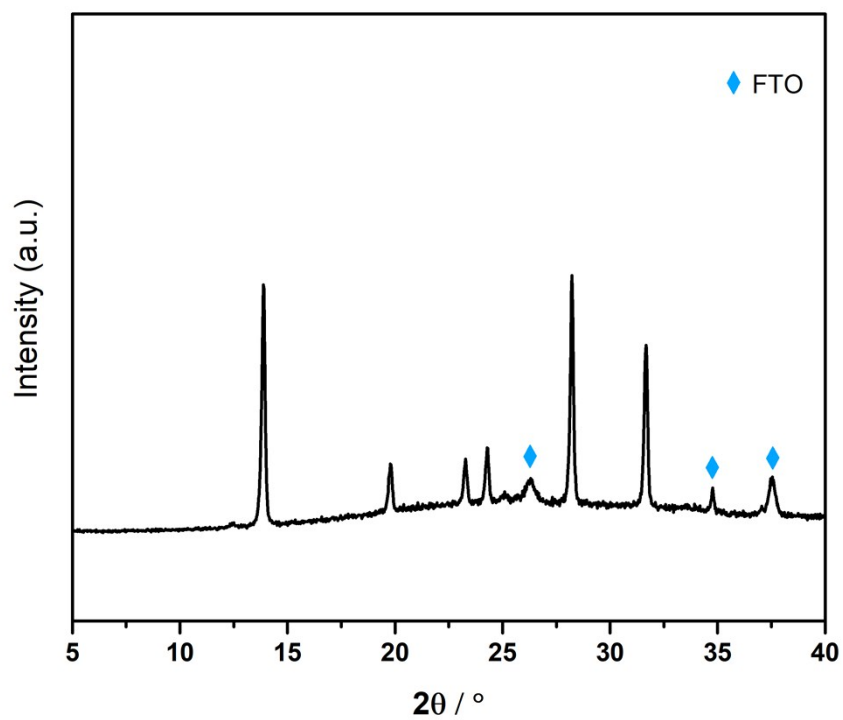


Figure S2. XRD of bulk MAPbI₃ film on FTO.

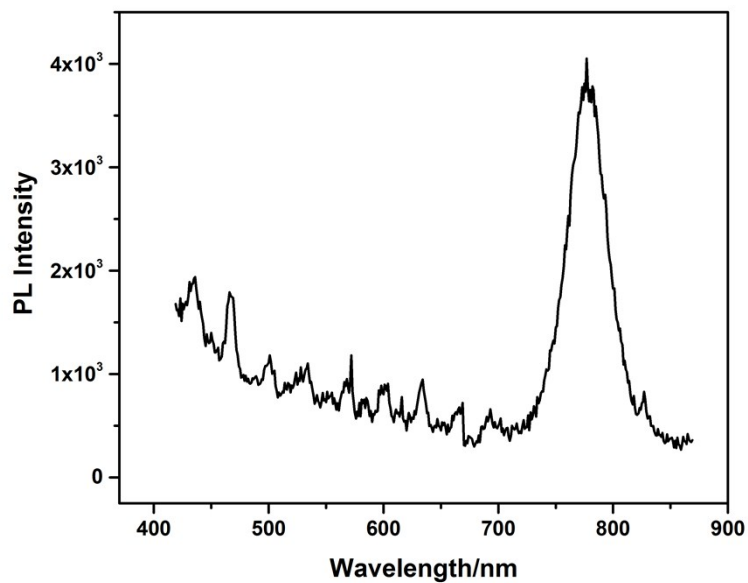


Figure S3. PL of bulk MAPbI₃ powder dispersed in toluene.

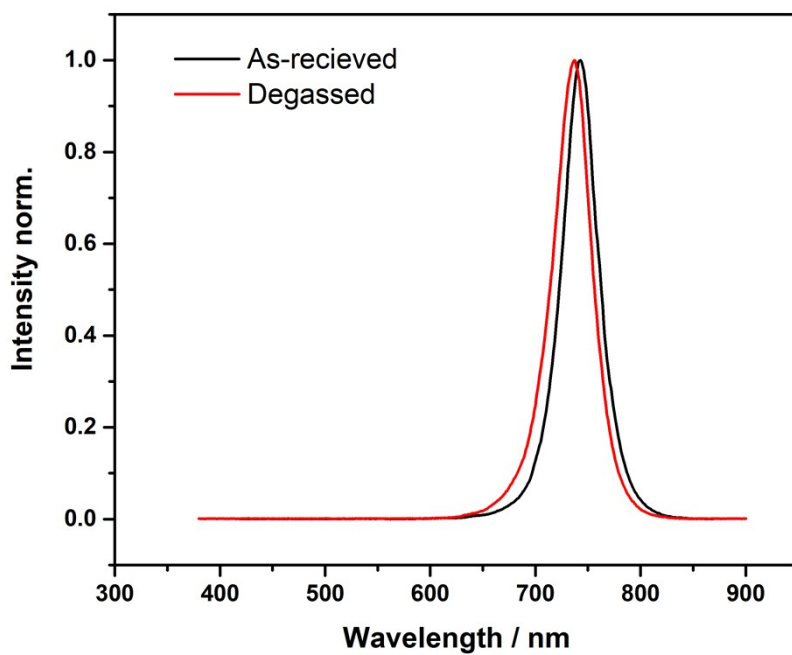


Figure S4. PL spectra of MAPbI₃ NCs made with degassed precursor solutions and as-received precursor solutions without degassing treatment. The PL of the degassed sample peaks at 737nm, with the FWHM of 42nm, while the peak of the non-degassed sample centered at 745nm with the FWHM of 39nm.

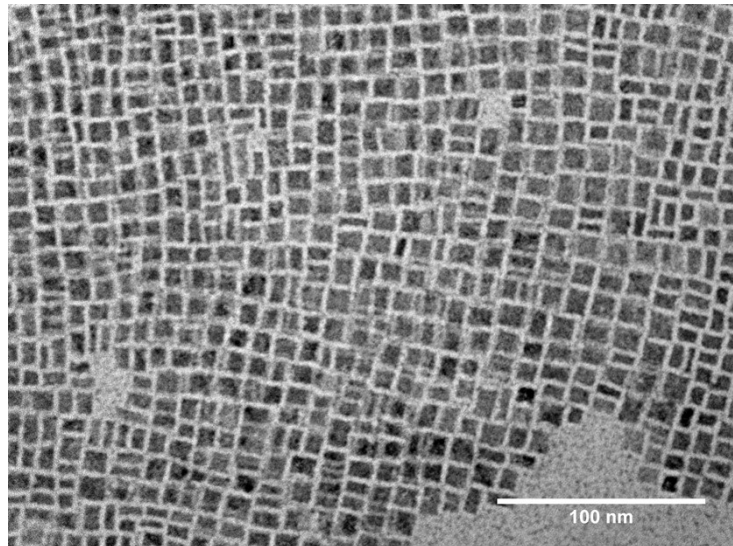


Figure S5. TEM image of MAPbI₃ nanoparticles prepared from degassed samples.

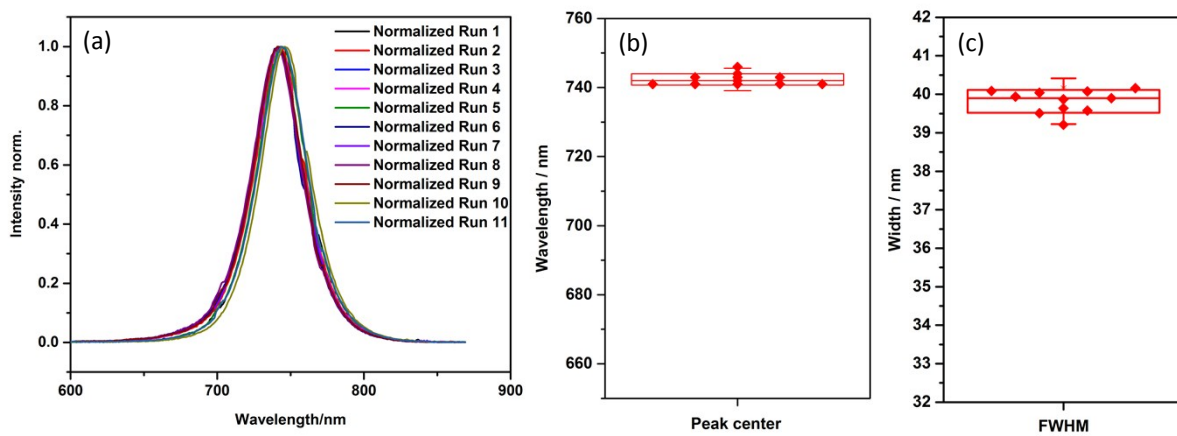


Figure S6. PL spectra (a) of MAPbI₃ NCs obtained in 11 different runs and the box plots of the (b) peak positions and (c) FWHM.

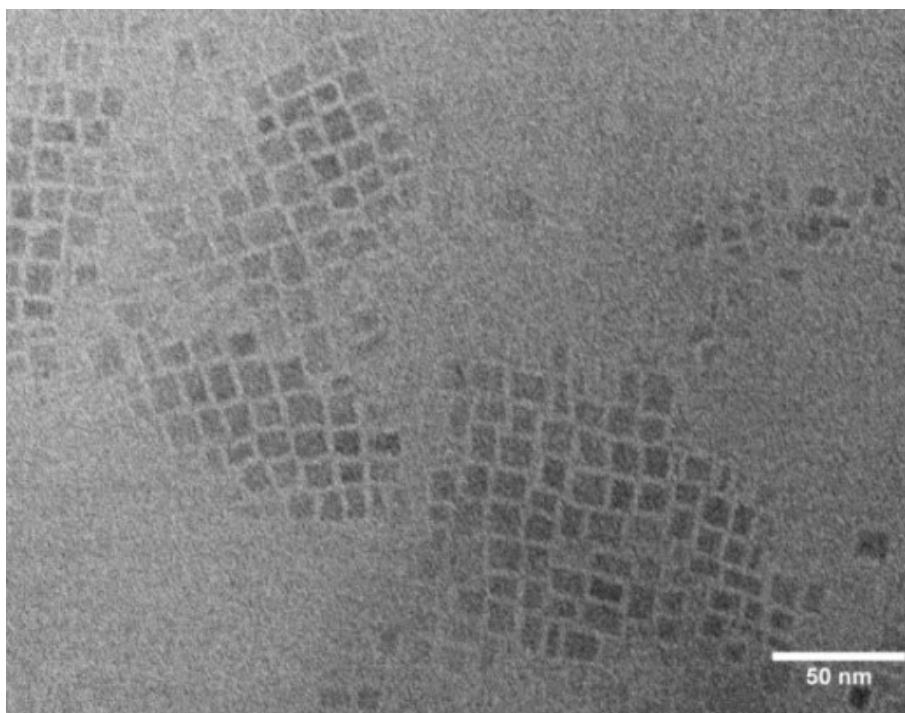


Figure S7. TEM images of the freshly made MAPbI₃ NCs.

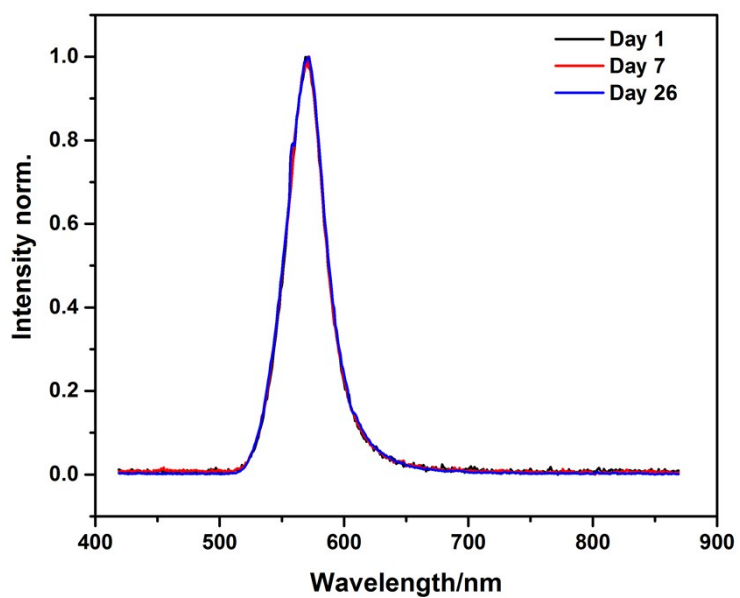


Figure S8. PL of MAPbI₃ NCs in toluene over 26 days.

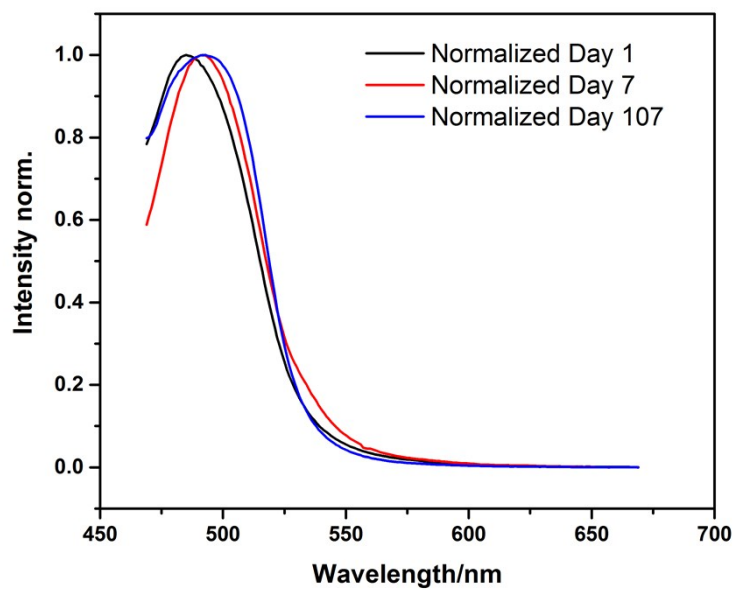


Figure S9. PL of MAPbBr₃ NCs in toluene over 107 days.

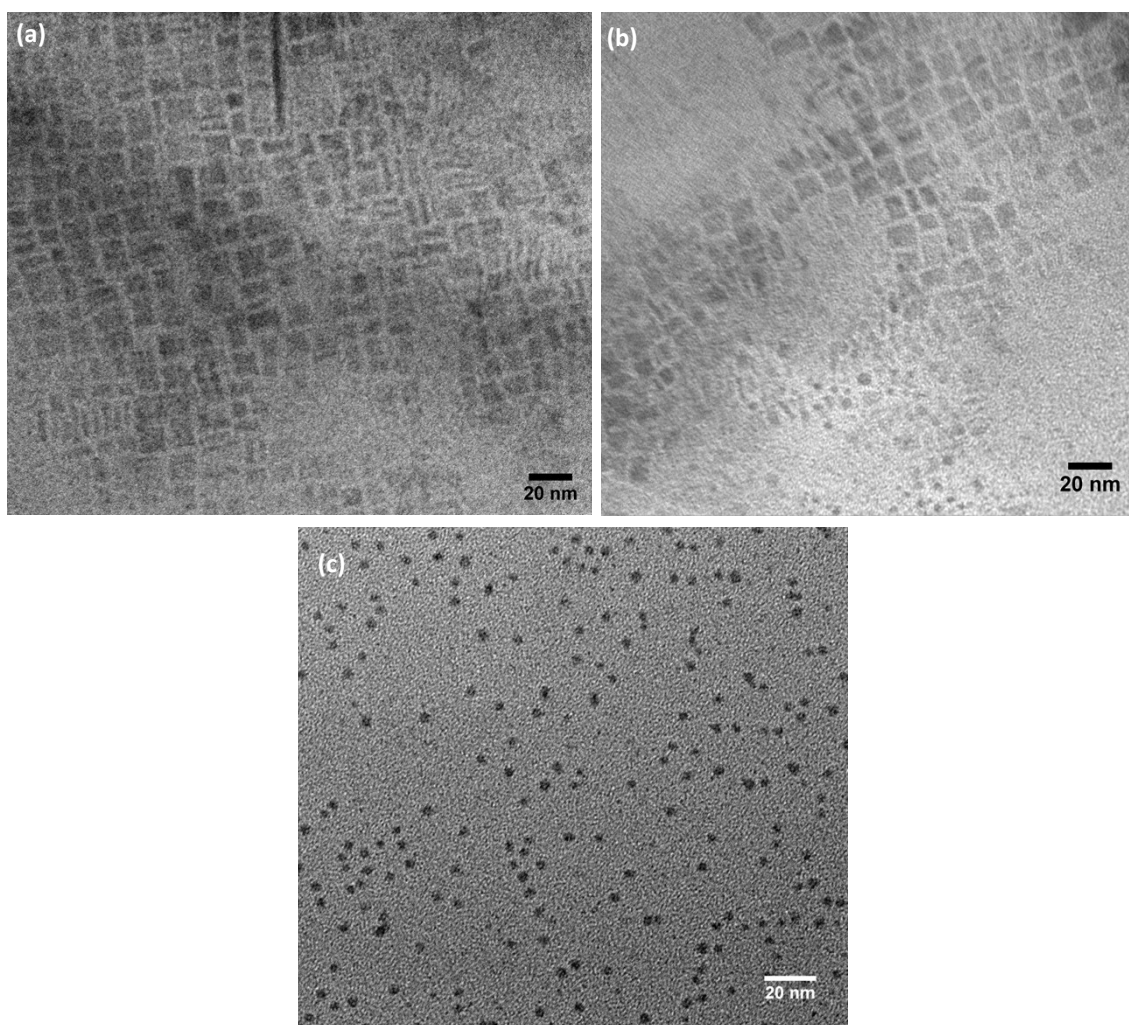


Figure S10. TEM images of (a) MAPbI₂Br, (b) MAPbI₂Br and (c) MAPbBr₃ NCs.

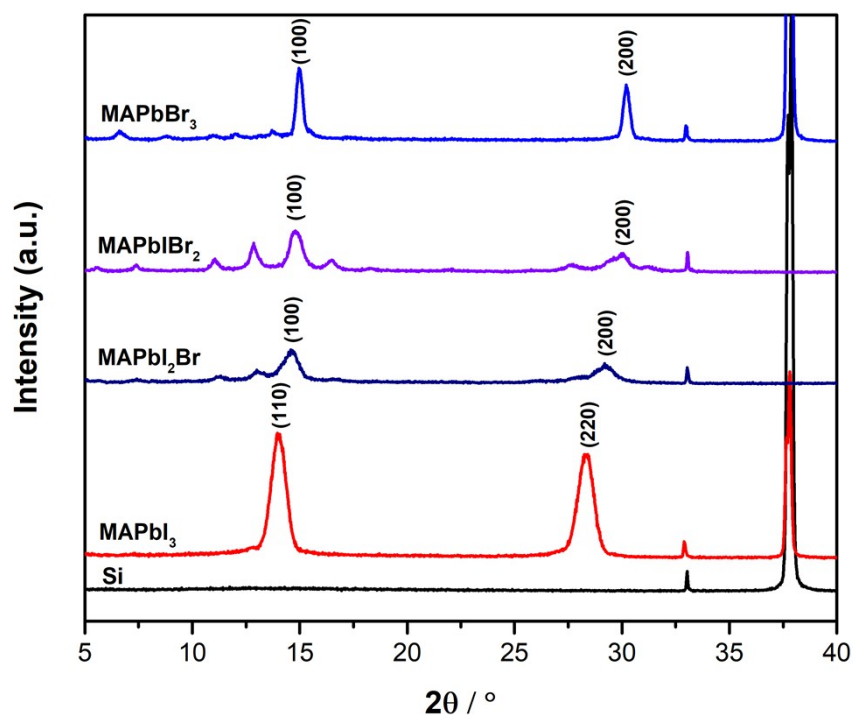


Figure S11. XRD patterns of MAPbX₃ NCs with different halide compositions. It shows the typical (110) and (220) reflections of the tetragonal phase merge upon increasing the bromide content to the (100) and (200) reflections of the cubic phase, which shift to higher angles with higher bromide content¹. The other unassigned small diffraction peaks in MAPbI₂Br, MAPbIBr₂ and MAPbBr₃ NCs could be due to the formation of 2D perovskite phase^{2, 3}.

Reference

1. S. A. Kulkarni, T. Baikie, P. P. Boix, N. Yantara, N. Mathews and S. Mhaisalkar, *Journal of Materials Chemistry A*, 2014, **2**, 9221-9225.
2. Y. Hassan, Y. Song, R. D. Pensack, A. I. Abdelrahman, Y. Kobayashi, M. A. Winnik and G. D. Scholes, *Advanced materials*, 2016, **28**, 566-573.
3. M. C. Weidman, M. Seitz, S. D. Stranks and W. A. Tisdale, *ACS Nano*, 2016, **10**, 7830-7839.